

Simulation study of BESIII with stitched CMOS pixel detector using ACTS*

Yi Liu,¹ Xiacong Ai,^{1,†} Guangyan Xiao,² Yaxuan Li,³ Linghui Wu,⁴ Liangliang Wang,⁴ Jianing Dong,⁵ Mingyi Dong,^{4,6} Qinglin Geng,⁵ Min Luo,⁷ Yan Niu,⁵ Anqing Wang,⁵ Chenxu Wang,⁷ Meng Wang,⁵ Lei Zhang,² Liang Zhang,⁵ Ruikai Zhang,⁷ Yao Zhang,⁴ Minggang Zhao,³ and Yang Zhou⁴

¹*School of Physics and Microelectronics, Zhengzhou University, Zhengzhou, Henan, 450001, China*

²*School of Physics, Nanjing University, Nanjing 210093, Jiangsu, China*

³*School of Physics, Nankai University, Tianjin 300071, China*

⁴*Institute of High Energy Physics, Chinese Academy of Sciences, 19B Yuquan Road, Shijingshan District, Beijing, China*

⁵*Research Center for Particle Science and Technology, Institute of Frontier and Interdisciplinary Science, Shandong University, Qingdao 266237, Shandong, China*

⁶*University of Chinese Academy of Sciences, 19A Yuquan Road, Shijingshan District, Beijing, China*

⁷*School of Information Science & Engineering, Harbin Institute of Technology, Weihai 264209, China*

Reconstruction of tracks of charged particles with high precision is very crucial for HEP experiments to achieve their physics goals. As the tracking detector of BESIII experiment, the BESIII drift chamber has suffered from aging effects resulting in degraded tracking performance after operation for about 15 years. To preserve and enhance the tracking performance of BESIII, one of the proposals is to add one layer of thin CMOS pixel sensor in cylindrical shape based on the state-of-the-art stitching technology, between the beam pipe and the drift chamber. The improvement of tracking performance of BESIII with such an additional pixel detector compared to that with only the existing drift chamber is studied using the modern common tracking software ACTS, which provides a set of detector-agnostic and highly performant tracking algorithms that have demonstrated promising performance for a few high energy physics and nuclear physics experiments.

Keywords: BESIII tracking detector, CMOS pixel sensor, Track reconstruction, Common tracking software

I. INTRODUCTION

The Beijing Spectrometer (BESIII) [1] at the Beijing Electron-Positron (BEPCII) Collider has been a great success producing prosperous physics results [2] in the τ -charm sector since 2009. However, after operation for about 15 years, the detectors at BESIII have been subjected to aging effects, which result in degraded performance of the detectors [3].

The tracking detector at BESIII is the Multilayer Drift Chamber (MDC), which provides measurement of momentum and position of the charged tracks, and information of energy loss in unit path length, i.e. dE/dx [4], of the charged tracks for particle identification. As shown in Ref. [3, 5], due to the beam-induced background with a hit rate up to 2 kHz/cm², the gain of the MDC cells in the first ten layers has shown an obvious decrease with a maximum decrease of about 39% for the innermost layer cells in 2017, which further leads to reduction of the spatial and momentum resolution of the charged tracks. Since BESIII is not expected to complete its mission in foreseen years [2, 3], the track reconstruction performance must be preserved and enhanced in order to not compromise the physics goals of BESIII, along with possible upgrade of the tracking system with state-of-the-art technologies for detection of charged particles. To get well prepared for the potential malfunction of the MDC due to aforementioned aging problem, plans of upgrading the BESIII inner tracker based on different technologies have been

proposed [3]. This includes replacement of the inner tracker with a new inner drift chamber [6] or a cylindrical gas electron multiplier (CGEM) tracker [7], which has attractive features such as high counting rate tolerance and low sensitivity to aging.

Compared to the gaseous detectors, the silicon pixel detector has excellent spatial resolution and good radiation resistance. Therefore, one of the additional options for the BESIII inner tracker upgrade is to use large-area thin Complementary Metal Oxide Semiconductor (CMOS) pixel sensor with good spatial resolution based on the cutting-edge stitching technology, which has already been used to produce CMOS pixel sensors for medical imaging applications [8–10]. Recently, the studies of designing a first wafer-scale stitched sensor prototype, the MOSS (Monolithic Stitched Sensor) chip, towards an improved vertex detector, i.e. the ITS3, at ALICE experiment, are presented in Ref. [11].

A Common Tracking Software (ACTS) [12] is a common High Energy Physics (HEP) software, providing a set of detector-agnostic, performant and modular tools for the track reconstruction in HEP using modern software technologies to facilitate concurrency, usability, maintenance and extendability to tackle the tracking challenges foreseen in HEP in future. So far, ACTS has been used for the track reconstruction at ATLAS [13], FASER [14], sPHENIX [15], STCF [16] etc., for different types of tracking detectors. In particular, promising tracking performance of ACTS for a tracking system with a drift chamber is firstly presented in Ref. [16].

In this study, the tracking performance of the BESIII MDC with an additional one-layer stitched cylindrical CMOS pixel detector inserted between the beam pipe and the inner wall of the MDC is studied using ACTS as the tracking software. The

* Supported by the National Natural Science Foundation of China (Nos. U2032203, 12275296, 12275297, 12075142, 12175256, 12035009) and National Key R&D Program of China (No. 2020YFA0406302)

† Corresponding author, xiaocongai@zzu.edu.cn

performance is compared to that of the current BESIII tracking detector with only the MDC based on the BESIII Offline Software System (BOSS) [17]. The manuscript is organized as follows. In Section II, the BESIII MDC and the proposed pixel detector based on the cylindrical CMOS pixel sensor are introduced. Section III introduces the tracking strategies in BOSS and ACTS. Improvement of the tracking performance at BESIII with an additional pixel detector is presented in Section IV. A brief conclusion is provided in Section V.

II. THE BESIII TRACKING DETECTOR AND STITCHED CMOS PIXEL DETECTOR

The BESIII MDC is a cylindrical chamber operating with a helium-based mixture gas ($\text{He}/\text{C}_3\text{H}_8 = 60:40$) and immersed in a 1 T magnetic field. The inner radius and outer radius of the MDC is 64 mm and 819 mm, respectively. The length of the wires ranges from 774 mm for the innermost layer to 2400 mm for the outermost layer. The drift cells which are almost square shaped are arranged in 43 circular layers, which alternate between the stereo layers and axial layers, i.e. in the order of 8 stereo layers, 12 axial layers, 16 stereo layers and 7 axial layers. The cell dimension is about $12 \text{ mm} \times 12 \text{ mm}$ for the 8 inner layers and $16.2 \text{ mm} \times 16.2 \text{ mm}$ for the 35 outer layers. The inner chamber is composed of the 8 inner layers and the outer chamber is composed of the 35 outer layers.

The CMOS pixel sensor has been widely used for vertex detectors in HEP, due to its excellent spatial resolution down to a few μm , tolerance of high hit rate up to 10^8 Hz/cm^2 , and good detection efficiency and radiation resistance. For example, the CMOS pixel sensor has been used for the inner tracker or vertex detector of the STAR experiment [18], the ALICE experiment [19] and the sPHENIX experiment [20]. It's also considered as a primary choice for the pixel sensor technology for the CEPC physics program [21]. Despite all the advantages of the CMOS pixel sensor, the tracking resolution of a traditional CMOS pixel detector, in particular for low momentum tracks, can be limited by the irreducible material budget of the support structure and cooling pipe, as shown in Ref. [22], where the MAPS-based CMOS pixel sensor is proposed for the upgrade of BESIII inner chamber. Therefore, tracking based on traditional CMOS pixel sensors can be challenging at BESIII, where tracks with transverse momentum down to 150 MeV are required to be reconstructed with good resolution.

In recent years, the innovative stitching technology emerged with the aim of producing large-area sensor in one wafer, which can be further thinned to about $50 \mu\text{m}$. With such thickness, the wafer can be curved into cylindrical shape, hence vastly simplifying the support structure and reducing the material budget. Based on such stitching technology, it's possible to construct a vertex detector using large-area thin CMOS pixel sensors with cylindrical shape and simplified support structure. As discussed in Ref. [11], the material budget per pixel layer is foreseen to be reduced to $0.05\% X_0$, to allow bending of the silicon. In this study, a vertex detector which consists of one layer of stitched cylindrical pixel

sensor with thickness of $50 \mu\text{m}$ ($0.05\% X_0$), as proposed in Ref. [11], and a length of 220 mm (including insensitive area within 7 mm to each end), resolution of $8.66 \mu\text{m}$ in the r - ϕ direction and $57.74 \mu\text{m}$ in the z direction, inserted between the beam pipe, which has a diameter of 63 mm [1], and the MDC inner wall, is considered. The stitching technology foresees cooling by air flow and no readout circuits in the active area. Therefore, the additional material budget from the cooling and readout infrastructure as well as the support structure in the active region of the pixel layer is expected to have a negligible impact on the tracking performance, and hence not taken into account in this study.

The geometry of the BESIII MDC and the pixel detector is shown in Figure 1.

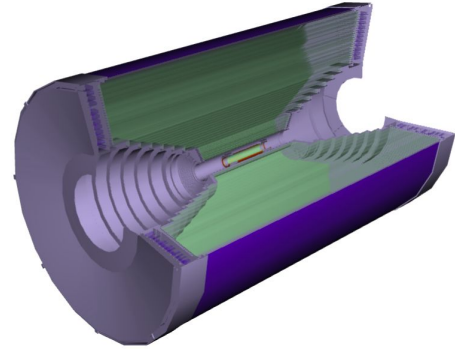


Fig. 1. A clipped view of geometry of the BESIII MDC (cell wires are shown in green colors) and the pixel detector (shown in orange color) outside of the beampipe.

III. TRACKING WITH BESIII OFFLINE SOFTWARE AND ACTS

The simulation study is based on samples generated using BOSS, which is the offline software framework for event generation, simulation, reconstruction, performance validation, physics analysis and visualization [23] for the BESIII experiment.

In BOSS, the production of both charmonium resonances and continuum process from the e^+e^- collisions is provided by the KKMC [24] generator and the decays of particles are modelled with EVTGEN [25], which can also be used to generate single particle samples. The detector description is based on the Geometry Description Markup Language (GDML) [26] and the interaction of particles with detectors is simulated with GEANT4 [27].

The performance of the BESIII MDC with the additional pixel detector is studied using the ACTS software, and compared to the performance of the BESIII MDC studied using the BESIII tracking software within BOSS. The workflow for

studies of the tracking performance is illustrated in Figure 2.

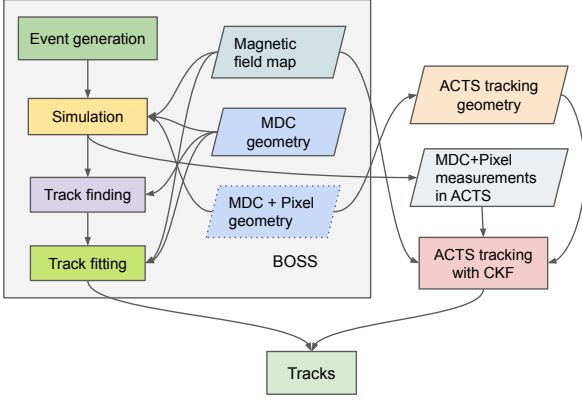


Fig. 2. The workflow of tracking performance studies based on BOSS and ACTS.

A. Tracking in BOSS

The trajectory of a charged particle in magnetic field is parameterized using the helix track parameters at BESIII, as described in Ref. [28]. Track finding and track fitting are two tasks in BOSS track reconstruction. Track finding is a pattern recognition problem of classifying measurements into subsets and creating track candidates, while track fitting is an estimation of the helix parameters. Two basic track finding algorithms are implemented in BOSS: the template matching algorithm (PAT) [29] and track segment finder algorithm (TSF) [28]. Both a specialized track finding method called TCurlFinder [30] and the global track finding method based on Hough transform (HOUGH) [31] have been implemented to salvage low transverse momentum tracks with $p_T < 0.12$ GeV. Besides, an extended segment construction scheme which can achieve higher efficiency for low transverse momentum tracks has been developed [32]. The found tracks using these algorithms are combined and fed into the Kalman Filter [33] algorithm for track fitting. Further track extrapolation is performed to obtain the track parameters at other subdetectors at BESIII.

B. Tracking with ACTS

A detailed introduction to ACTS, including geometry description, parameterization of track parameters and measurements, and tracking algorithms etc., can be found in Ref. [12]. The implementation of ACTS for track reconstruction for the BESIII tracking detector is outlined below.

To use ACTS for track reconstruction, the detector geometry with detailed description of detector material and placement, e.g. the GEANT4-based detector geometry, needs to be

transformed into ACTS internal geometry, i.e. ACTS tracking geometry, which has a simplified description of the passive detector material to facilitate fast navigation and track reconstruction. The TGEO [34] plugin in ACTS is used to transform the TGEO version of the BESIII detector geometry, which is created based on GDML exported from the GEANT4-based geometry, into ACTS tracking geometry with material mapped to the auxiliary surfaces. The one pixel layer of the pixel detector is converted to a cylinder surface in ACTS and the 43 layers of signal wires of the MDC are converted to 43 layers of line surfaces, dedicated to representation of measurements for a drift chamber or track parameters at the interaction point³, in ACTS.

The hits on the MDC after digitization are transformed into one-dimensional measurements associated to the line surfaces in ACTS describing the drift distance of a drift chamber. The hits on the pixel detector after simulation are transformed into two-dimensional measurements by smearing the simulated hits with the resolution of the pixel detector using Gaussian functions. Those measurements are associated to the ACTS cylinder surfaces, where the local x (y) coordinate represents the $r \cdot \varphi$ (z) in the cylinder frame, i.e. r represents the radius of the cylinder, φ represents the azimuthal angle of the position on the cylinder and z is the coordinate in the z direction.

The BESIII magnetic field is transformed into ACTS interpolated magnetic field using the field map of BESIII magnetic field. With an interpolated field provider in ACTS, the value of the magnetic field for any given position is calculated by interpolating from a grid of known values, e.g. eight corner points of a field cell in three-dimensional coordinate system.

The track fitting and finding is performed simultaneously using the combinatorial Kalman Filter [35] algorithm in ACTS, which has the capability of rejecting noise hits based on the χ^2 calculated using the distance between the hit and the predicted track parameters, and the covariance of the hit and the predicted track parameters. If multiple hits are found to be compatible with the predicted track parameters, the hit with the best χ^2 is used to filter the track parameters. The smoothed track parameters at the first measurement are eventually extrapolated to the beam line to obtain the estimated track parameters at the interaction point.

IV. TRACKING PERFORMANCE STUDIES

A. Monte-Carlo sample generation

The impact of the pixel detector on the resolution of the track parameters is studied using single μ^- and single π^- samples. The samples are generated with fixed transverse momentum p_T , $\cos\theta$ (θ is the polar angle) uniformly distributed between $[-0.8, 0.8]$, and azimuthal angle ϕ uniformly distributed in the range of $[0, 2\pi]$. The impact of

³ Suppose the wire has a direction of \vec{w} and the track direction is \vec{t} in the global coordinate frame, the x axis and y axis in the local coordinate frame of a line surface is $\vec{w} \times \vec{t}$ and \vec{w} , respectively.

the pixel detector on the tracking efficiency is studied using $\psi(3686) \rightarrow \pi^+\pi^- J/\psi, J/\psi \rightarrow \mu^+\mu^-$ events generated at $\sqrt{s} = 3.686$ GeV. The two-dimensional distributions of $\cos\theta$ and p_T for μ and π in this process are shown in Figure 3.

The random background hits in the MDC due to beam related background or electronic noises are generated in the standard simulation sample production at BESIII. Since dedicated background noise model for the pixel detector is not available yet, no background noise is considered for the inserted pixel layer in this study.

B. Track reconstruction performance

The resolution of the impact track parameters, d_0 , d_z and the relative resolution of the transverse momentum p_T as a function of p_T for the BESIII MDC with an additional pixel layer, which is placed with the radius r_{pixel} at three different values, i.e. 35 mm, 45 mm or 55 mm, compared to those of BESIII MDC, are shown in Figure 4. While r_{pixel} has little impact on the resolution of p_T , the spatial resolution is better with smaller r_{pixel} . With $r_{\text{pixel}} = 35$ mm, the resolution of d_0 and d_z is 60 μm and 120 μm for μ^- and π^- with $p_T = 1$ GeV, respectively, and the relative resolution of 44% for p_T at $p_T = 1$ GeV is achieved. The resolution of d_0 , d_z , p_T can be improved by up to 67%, 93% and 32%, respectively, if the proposed Pixel detector is added to the current BESIII tracking detector.

The comparison of the tracking efficiency, which is defined as the ratio of generated charged particles which have corresponding reconstructed track in the detector region ($|\cos\theta| < 0.93$), between the BESIII MDC with the additional pixel layer and the BESIII MDC only is shown in Figure 5. The additional pixel layer can significantly improve the tracking efficiency for tracks with in particular low momentum or large $|\cos\theta|$. For μ with p_T below 0.6 GeV in the $\psi(3686) \rightarrow \pi^+\pi^- J/\psi, J/\psi \rightarrow \mu^+\mu^-$ process, the improvement can reach 9%. The improvement can reach 10% for π with $0.85 < |\cos\theta| < 0.93$. The pixel with $r_{\text{pixel}} = 35$ mm provides better

tracking efficiency than other two choices.

V. CONCLUSION

After operation for about 15 years, the tracking detector of BESIII experiment has suffered from aging effects and needs to be upgraded to preserve its tracking performance for BESIII to fulfill its remaining physics goals in the next few years. The possibility of inserting a one-layer pixel detector using the large-area thin CMOS pixel sensor in cylindrical shape based on the stitching technology, between the beam pipe and the MDC, was considered. The spatial and momentum resolution was studied using ACTS and compared to the performance of the current BESIII tracking detector obtained using the BESIII offline software. The proposal based on the stitched cylindrical CMOS pixel sensor was found to be very promising, i.e. the resolution of d_0 , d_z , p_T can be improved by up to 67%, 93% and 32%, respectively, and the tracking efficiency for particles in the $\psi(3686) \rightarrow \pi^+\pi^- J/\psi, J/\psi \rightarrow \mu^+\mu^-$ events can be improved by up to 10% in the low p_T or large $|\cos\theta|$ region, with the additional pixel layer placed at an radius of 35 mm. Meanwhile, it's the first time that ACTS was used for track reconstruction for a drift chamber with calibrated measurements and realistic noise hits. In future studies, the noise model of this state-of-the-art pixel detector will be studied and the tracking performance taking into account the noise on the pixel detector will be investigated.

ACKNOWLEDGMENTS

This work is supported in part by National Natural Science Foundation of China (NSFC) under Contracts Nos. U2032203, 12275296, 12275297, 12075142, 12175256, 12035009 and National Key R&D Program of China under Grants No. 2020YFA0406302.

-
- [1] M. Ablikim, et al., Design and construction of the BESIII detector, Nucl. Instrum. Meth. A 614 (3) (2010) 345–399. doi:<https://doi.org/10.1016/j.nima.2009.12.050>.
 - [2] C.-Z. Yuan, S. L. Olsen, The BESIII physics programme, Nature Reviews Physics 1 (8) (2019) 480–494. doi:[10.1038/s42254-019-0082-y](https://doi.org/10.1038/s42254-019-0082-y).
 - [3] M. Ablikim, et al., Future Physics Programme of BESIII *, Chinese Physics C 44 (4) (2020) 040001. doi:[10.1088/1674-1137/44/4/040001](https://doi.org/10.1088/1674-1137/44/4/040001).
 - [4] C. Xue-Xiang, et al., Studies of dE/dx measurements with the BESIII, Chinese Physics C 34 (12) (2010) 1852. doi:[10.1088/1674-1137/34/12/012](https://doi.org/10.1088/1674-1137/34/12/012).
 - [5] M.-Y. Dong, Q.-L. Xiu, L.-H. Wu, Z. Wu, Z.-H. Qin, P. Shen, F.-F. An, X.-D. Ju, Y. Liu, K. Zhu, Q. Ou-Yang, Y.-B. Chen, Aging effect in the BESIII drift chamber*, Chinese Physics C 40 (1) (2016) 016001. doi:[10.1088/1674-1137/40/1/016001](https://doi.org/10.1088/1674-1137/40/1/016001).
 - [6] Y.-J. Xie, et al., Construction and cosmic-ray test of the new inner drift chamber for BESIII, Chinese Physics C 40 (9) (2016) 096003. doi:[10.1088/1674-1137/40/9/096003](https://doi.org/10.1088/1674-1137/40/9/096003).
 - [7] A. Bortone, Development and operation of the CGEM Inner Tracker for the BESIII experiment, Nuclear Instruments and Methods in Physics Research Section A: Accelerators, Spectrometers, Detectors and Associated Equipment 1048 (2023) 167957. doi:<https://doi.org/10.1016/j.nima.2022.167957>.
 - [8] S. Bohndiek, A. Blue, J. Cabello, A. Clark, N. Guerrini, P. Evans, E. Harris, A. Konstantinidis, D. Maneuski, J. Osmond, V. O'Shea, R. Speller, R. Turchetta, K. Wells, H. Zin, N. Allinson, Characterization and Testing of LAS: A Prototype 'Large Area Sensor' With Performance Characteristics Suit-

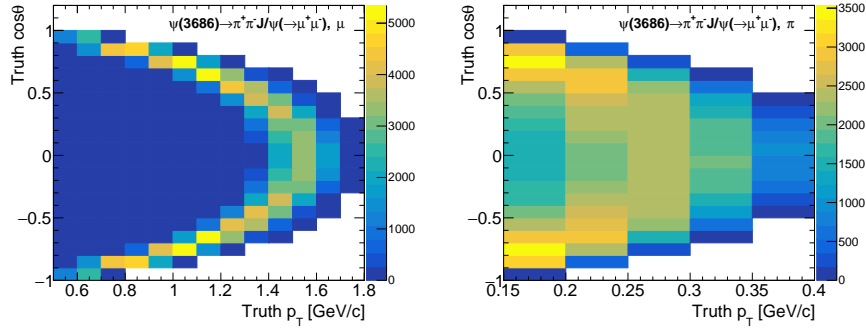


Fig. 3. The distributions of $\cos\theta$ versus p_T for μ (left) and π (right) generated in $\psi(3686) \rightarrow \pi^+\pi^- J/\psi$, $J/\psi \rightarrow \mu^+\mu^-$ events.

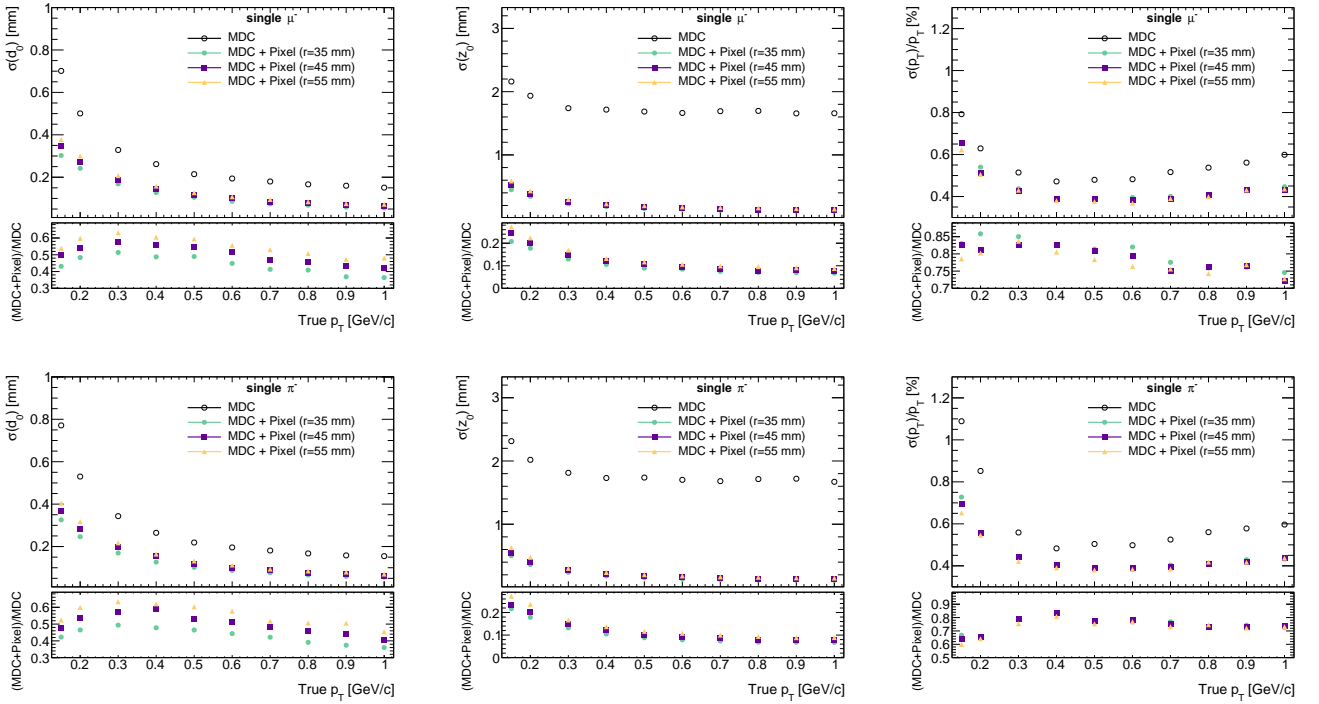


Fig. 4. The resolution of d_0 (left), z_0 (middle) and relative resolution of p_T (right) for single μ^- (top) and single π^- (bottom) as a function of particle p_T for the BESIII MDC only (black circle), and BESIII MDC with an additional pixel layer (denoted as "Pixel") placed with $r_{\text{pixel}} = 35$ mm (blue dot), 45 mm (purple triangle) and 55 mm (yellow triangle), respectively.

- able for Medical Imaging Applications, Nuclear Science, IEEE Transactions on 56 (2009) 2938 – 2946. [doi:10.1109/TNS.2009.2029575](https://doi.org/10.1109/TNS.2009.2029575).
- [9] A. Konstantinidis, M. Szafraniec, R. Speller, A. Olivo, The Dexela 2923 CMOS X-ray detector: A flat panel detector based on CMOS active pixel sensors for medical imaging applications, Nuclear Instruments and Methods in Physics Research Section A: Accelerators, Spectrometers, Detectors and Associated Equipment 689 (2012) 12–21. [doi:10.1016/j.nima.2012.06.024](https://doi.org/10.1016/j.nima.2012.06.024).
- [10] M. Farrier, T. Achterkirchen, G. Weckler, A. Mrozack, Very Large Area CMOS Active-Pixel Sensor for Digital Radiography, Electron Devices, IEEE Transactions on 56 (2009) 2623 – 2631. [doi:10.1109/TED.2009.2031001](https://doi.org/10.1109/TED.2009.2031001).
- [11] G. Aglieri Rinella, Developments of stitched monolithic pixel sensors towards the ALICE ITS3, Nuclear Instruments and Methods in Physics Research Section A: Accelerators, Spectrometers, Detectors and Associated Equipment 1049 (2023) 168018. [doi:https://doi.org/10.1016/j.nima.2023.168018](https://doi.org/10.1016/j.nima.2023.168018).
- [12] X. Ai, et al., A Common Tracking Software Project, Computing and Software for Big Science 6 (1) (2022) 8. [doi:10.1007/s41781-021-00078-8](https://doi.org/10.1007/s41781-021-00078-8).
- [13] ATLAS Collaboration, Software Performance of the ATLAS Track Reconstruction for LHC Run 3, Tech. rep., CERN, Geneva, all figures including auxiliary figures are available at <https://atlas.web.cern.ch/Atlas/GROUPS/PHYSICS/PUBNOTES/ATL-PHYS-PUB-2021-012> (May 2021).

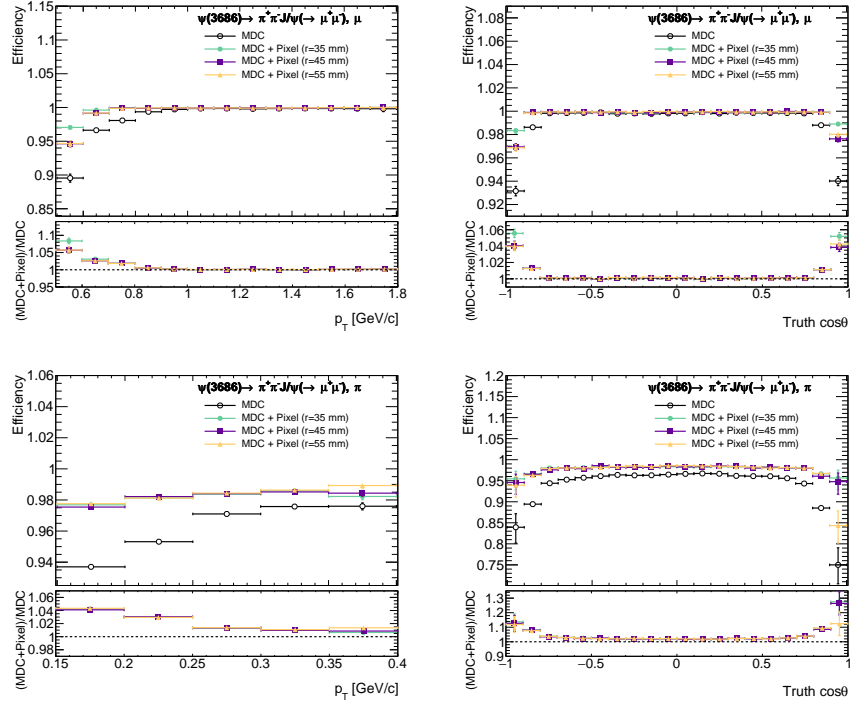


Fig. 5. The tracking efficiency of μ (top), π (bottom) in the process of $\psi(3686) \rightarrow \pi^+\pi^-J/\psi$, $J/\psi \rightarrow \mu^+\mu^-$ as a function of particle p_T (left) and $\cos\theta$ (right) for the BESIII MDC only (black circle), and BESIII MDC with an additional pixel layer (denoted as "Pixel") placed with $r_{\text{pixel}} = 35$ mm (blue dot), 45 mm (purple triangle) and 55 mm (yellow triangle), respectively.

- [14] H. Abreu, et al., First Direct Observation of Collider Neutrinos with FASER at the LHC, *Phys. Rev. Lett.* 131 (2023) 031801. [doi:10.1103/PhysRevLett.131.031801](https://doi.org/10.1103/PhysRevLett.131.031801).
- [15] J. D. Osborn, A. D. Frawley, J. Huang, S. Lee, H. P. D. Costa, M. Peters, C. Pinkenburg, C. Roland, H. Yu, Implementation of ACTS into sPHENIX Track Reconstruction, *Computing and Software for Big Science* 5 (1) (2021) 23. [doi:10.1007/s41781-021-00068-w](https://doi.org/10.1007/s41781-021-00068-w).
- [16] X. Ai, X. Huang, Y. Liu, Implementation of ACTS for STCF track reconstruction, *Journal of Instrumentation* 18 (07) (2023) P07026. [doi:10.1088/1748-0221/18/07/P07026](https://doi.org/10.1088/1748-0221/18/07/P07026).
- [17] BESIII Offline Software System, <https://bes3.readthedocs.io/index.html>.
- [18] A. Dorokhov, G. Bertolone, J. Baudot, C. Colledani, G. Claus, Y. Degerli, R. De Masi, M. Deveau, G. Dozière, W. Dulinski, M. Gélin, M. Goffe, A. Himmi, C. Hu-Guo, K. Jaaskelainen, M. Koziel, F. Morel, C. Santos, M. Specht, I. Valin, G. Voutsinas, M. Winter, High resistivity CMOS pixel sensors and their application to the STAR PXL detector, *Nuclear Instruments and Methods in Physics Research Section A: Accelerators, Spectrometers, Detectors and Associated Equipment* 650 (1) (2011) 174–177, international Workshop on Semiconductor Pixel Detectors for Particles and Imaging 2010. [doi:https://doi.org/10.1016/j.nima.2010.12.112](https://doi.org/10.1016/j.nima.2010.12.112).
- [19] G. Aglieri Rinella, The ALPIDE pixel sensor chip for the upgrade of the ALICE Inner Tracking System, *Nuclear Instruments and Methods in Physics Research Section A: Accelerators, Spectrometers, Detectors and Associated Equipment* 845 (2017) 583–587, proceedings of the Vienna Conference on Instrumentation 2016. [doi:https://doi.org/10.1016/j.nima.2016.05.016](https://doi.org/10.1016/j.nima.2016.05.016).
- [20] Y. Ji, Heavy flavor physics with the sphenix maps vertex tracker upgrade, *Nuclear Physics A* 1005 (2021) 121792, the 28th International Conference on Ultra-relativistic Nucleus-Nucleus Collisions: Quark Matter 2019. [doi:https://doi.org/10.1016/j.nuclphysa.2020.121792](https://doi.org/10.1016/j.nuclphysa.2020.121792).
- [21] S. Dong, P. Yang, Y. Zhang, Y. Zhou, H. Wang, L. Xiao, L. Zhang, Z. Shi, D. Guo, Z. Wu, J. Dong, Y. Lu, X. Sun, Q. Ouyang, Design and characterisation of the JadePix-3 CMOS pixel sensor, *Nuclear Instruments and Methods in Physics Research Section A: Accelerators, Spectrometers, Detectors and Associated Equipment* 1048 (2023) 167967. [doi:https://doi.org/10.1016/j.nima.2022.167967](https://doi.org/10.1016/j.nima.2022.167967).
- [22] M. Dong, X. Ju, X. Tian, X. Lu, C. Qu, Q. Xiu, X. Ma, J. Dong, H. Zhang, L. Wu, X. Jiang, Q. OuYang, M. Wang, Development of maps-based detector ladders for the besiii inner tracker upgrade, *Nuclear Instruments and Methods in Physics Research Section A: Accelerators, Spectrometers, Detectors and Associated Equipment* 924 (2019) 287–292, 11th International Hiroshima Symposium on Development and Application of Semiconductor Tracking Detectors. [doi:https://doi.org/10.1016/j.nima.2018.06.032](https://doi.org/10.1016/j.nima.2018.06.032).
- [23] K.-X. Huang, Z.-J. Li, Z. Qian, J. Zhu, H.-Y. Li, Y.-M. Zhang, S.-S. Sun, Z.-Y. You, Method for detector description transformation to unity and application in besiii, *Nuclear Science and Techniques* 33 (11) (2022) 142. [doi:10.1007/s41365-022-01133-8](https://doi.org/10.1007/s41365-022-01133-8).
- [24] S. Jadach, B. F. L. Ward, Z. Wař, Coherent exclusive exponentiation for precision Monte Carlo calculations, *Phys. Rev. D* 63 (2001) 113009. [doi:10.1103/PhysRevD.63.113009](https://doi.org/10.1103/PhysRevD.63.113009).

- [25] D. J. Lange, The EvtGen particle decay simulation package, Nucl. Instrum. Meth. A 462 (1) (2001) 152–155, bEAUTY2000, Proceedings of the 7th Int. Conf. on B-Physics at Hadron Machines. doi:[https://doi.org/10.1016/S0168-9002\(01\)00089-4](https://doi.org/10.1016/S0168-9002(01)00089-4).
- [26] Geometry Description Markup Language (GDML), <https://gdml.web.cern.ch/GDML>.
- [27] S. Agostinelli, et al., Geant4—a simulation toolkit, Nucl. Instrum. Meth. A 506 (3) (2003) 250–303. doi:[https://doi.org/10.1016/S0168-9002\(03\)01368-8](https://doi.org/10.1016/S0168-9002(03)01368-8).
- [28] Q.-G. Liu, et al., Track reconstruction using the TSF method for the BESIII main drift chamber, Chinese Physics C 32 (7) (2008) 565. doi:[10.1088/1674-1137/32/7/011](https://doi.org/10.1088/1674-1137/32/7/011).
- [29] Y. Zhang, et al., Pattern-Matching Track Reconstruction for the BESIII Main Drift Chamber, HIGH ENERGY PHYSICS AND NUCLEAR PHYSICS 31 (06) (2007) 570–575.
- [30] L.-K. Jia, et al., Study of low momentum track reconstruction for the BESIII main drift chamber, Chinese Physics C 34 (12) (2010) 1866. doi:[10.1088/1674-1137/34/12/014](https://doi.org/10.1088/1674-1137/34/12/014).
- [31] J. Zhang, et al., Low transverse momentum track reconstruction based on the Hough transform for the BESIII drift chamber, Radiation Detection Technology and Methods 1 (2) (5 2018). doi:[10.1007/s41605-018-0052-4](https://doi.org/10.1007/s41605-018-0052-4).
- [32] C.-L. Ma, et al., An extended segment pattern dictionary for a pattern matching tracking algorithm at BESIII, Chinese Physics C 37 (6) (2013) 066202. doi:[10.1088/1674-1137/37/6/066202](https://doi.org/10.1088/1674-1137/37/6/066202).
- [33] J.-K. Wang, et al., Besiii track fitting algorithm, Chinese Physics C 33 (10) (2009) 870. doi:[10.1088/1674-1137/33/10/010](https://doi.org/10.1088/1674-1137/33/10/010).
- [34] R. Brun, A. Gheata, M. Gheata, The ROOT geometry package, Nucl. Instrum. Methods. Phys. Res. A 502 (2) (2003) 676–680. doi:[10.1016/S0168-9002\(03\)00541-2](https://doi.org/10.1016/S0168-9002(03)00541-2).
- [35] R. Frühwirth, A. Strandlie, Track Finding, Springer International Publishing, Cham, 2021, pp. 81–102. doi:[10.1007/978-3-030-65771-0_5](https://doi.org/10.1007/978-3-030-65771-0_5).